electronics

MDPI

Article

Electron Affinity and Bandgap Optimization of Zinc Oxide for Improved Performance of ZnO/Si Heterojunction Solar Cell Using PC1D Simulations

Babar Hussain [1,*], Aasma Aslam [2], Taj M Khan [3,4], Michael Creighton [1] and Bahman Zohuri [2]

1 Intel Corporation, Rio Rancho, NM 87124, USA; michaelcreighton38@gmail.com
2 Department of Electrical and Computer Engineering, The University of New Mexico, Albuquerque, NM 87131, USA; aasmaaslam@yahoo.com (A.A.); zohurib@unm.edu (B.Z.)
3 School of Physics, Trinity College Dublin, Dublin 2, Ireland; tajakashne@gmail.com
4 National Institute of Lasers and Optronics, Islamabad 45650, Pakistan
* Correspondence: babarhussain2002@hotmail.com

Received: 26 December 2018; Accepted: 14 February 2019; Published: 20 February 2019

Abstract: For further uptake in the solar cell industry, n-ZnO/p-Si single heterojunction solar cell has attracted much attention of the research community in recent years. This paper reports the influence of bandgap and/or electron affinity tuning of zinc oxide on the performance of n-ZnO/p-Si single heterojunction photovoltaic cell using PC1D simulations. The simulation results reveal that the open circuit voltage and fill factor can be improved significantly by optimizing valence-band and conduction-band off-sets by engineering the bandgap and electron affinity of zinc oxide. An overall conversion efficiency of more than 20.3% can be achieved without additional cost or any change in device structure. It has been found that the improvement in efficiency is mainly due to reduction in conduction band offset that has a significant influence on minority carrier current.

Keywords: zinc oxide; silicon; ZnO/Si; electron affinity; bandgap tuning; conduction band offset; heterojunction; solar cells; PC1D

1. Introduction

Zinc oxide (ZnO) is an emerging material in the semiconductor industry due to its abundance and being environmentally friendly. The only major drawback of ZnO that hinders its use in the fabrication of a homojunction device is that it cannot be p-doped reliably and reproducibly. However, n-ZnO has been found to have applications in several optoelectronic devices, such as photovoltaic cells [1]. Since the proposed use of n-ZnO as an emitter layer and antireflection (AR) coating, several researchers have employed n-ZnO thin films to fabricate potentially high efficiency and low-cost solar cells [2–4]. Apart from several other properties which make ZnO a unique wide bandgap material, its bandgap and electron affinity can be tuned over a large range by doping or alloying. Recently, nickel (Ni) doped ZnO thin films were prepared using spray pyrolysis and an optical bandgap decrease from 3.47 eV for the undoped ZnO film to 2.87 eV for 15% Ni doping was achieved [5]. In 2010, Mayer et al. demonstrated that the bandgap of ZnO prepared using pulsed laser deposition can be narrowed down to 2 eV by Se incorporation [6]. Later, the same research group reported effects of growth parameters on the electron affinity of ZnO [7]. Furthermore, there are various reports available demonstrating significant reduction in conduction band offset (or electron affinity) by incorporating magnesium (Mg) in ZnO. We have previously reported synthesis of ZnO thin films using metal organic chemical vapor deposition (MOCVD) with optimized parameters for the fabrication of a n-ZnO/p-Si solar cell [1]. It was anticipated that an overall conversion efficiency of 19% and fill factor of 81% can be achieved using the proposed structure. Following this, several groups reported

different experimental results [8–12] for the n-ZnO/p-Si solar cell with the best efficiency of 14% achieved by Pietruszka et al. recently [13]. Also, few groups have recently reported simulation results optimizing different parameters of ZnO/Si solar cell. Chen et al. investigated the influence of ZnO thickness, buffer layer and work function of electrodes on the performance of ZnO/Si solar cell using AFORS-HET tool and proved that the conversion efficiency of 17.16% can be achieved [10]. Ziani and Belkaid reported similar performance of ZnO/Si solar cell using SCAPS-1D software [14]. Very recently, Vallisree et al. used Silvaco ATLAS simulator and reported that efficiency up to 14.46% can be achieved by incorporation of Mg in ZnO [15]. Askari et al. provided an interesting study on the interface properties of ZnO/Si heterojunction and computed ~14% efficiency of ZnO/Si solar cell using TCAD simulations [16]. The ZnO/Si heterojunction solar cell is a relatively new idea and there is no study available that reports optimized values of electron affinity and bandgap of ZnO, which dictate conduction- and valence-band offsets, to achieve best performance of the solar cell.

In this paper, we report simulation based optimization of bandgap and electron affinity of ZnO to enhance the conversion efficiency of a ZnO/Si single heterojunction solar cell. The schematic of the solar cell structure is depicted in Figure 1. The effects of valence-band and conduction-band off-set engineering on the open circuit voltage (V_{OC}), short circuit current density (J_{SC}), fill factor (FF), and overall conversion efficiency (η) have been investigated using PC1D software. The simulations prove that the conversion efficiency as high as 20.3% can be obtained from ZnO/Si solar cell.

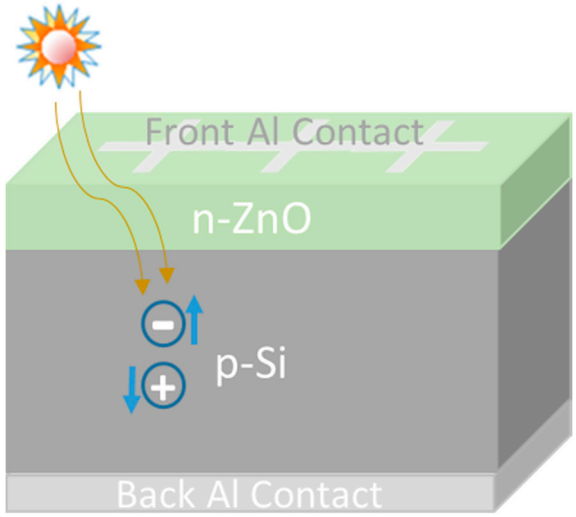

Figure 1. Schematic of the n-ZnO/p-Si single heterojunction solar cell structure.

2. Background

The energy band diagram of an ideal n-ZnO/p-Si heterojunction is depicted in Figure 2, which appears similar to a type-II heterojunction. The features of the band alignment are determined based on the Anderson energy-band rule also known as the electron affinity model. The conduction band offset (ΔE_C) and valence band offset (ΔE_V) according to Anderson's rule are given by

$$\Delta E_C = \chi_2 - \chi_1 \quad (1)$$

$$\Delta E_V = (\chi_2 + E_{g2}) - (\chi_1 + E_{g1}), \quad (2)$$

where χ is electron affinity, E_g is bandgap, and subscripts 1 and 2 correspond to Si and ZnO, respectively in our case. The electron affinity and bandgap of Si are well known to be 4.05 and 1.12 eV, respectively. These values vary significantly in literature for ZnO. Actually, the bandgap of ZnO can be tuned over a large range from 3 to 5 eV by alloying, which is considered as one of the unique advantages of ZnO. Sundaram et al. have reported the electron affinity of ZnO to be around 4.5 eV, which was calculated using I-V measurements and the Shottky-Mott model [17]. Since the ZnO films are highly

doped, their fermi level almost overlaps with the conduction band edge. Therefore, the work function of ZnO is considered the same as electron affinity. These values result in ΔE_C and ΔE_V of ~0.4 eV and 2.55 eV, respectively. Sundaram et al. have also considered a very thin (1–2 nm) oxide layer at the interface that is likely to develop due to high energy process like magnetron sputtering [18,19]. The carrier flow across the junction is largely affected by oxide layer thickness, which dictates the tunneling coefficient [20].

There are two limitations of Anderson's rule [21]. The first is that Anderson's rule neglects the electron correlation effect. The correlation effect occurs when the electron moves to the vacuum level (according to the definition of electron affinity) and surrounding electrons rearrange themselves to reduce the total energy of the system. The magnitude of the correlation effect is generally very small. The second drawback is the lack of consideration of lattice mismatch and interface defects. Dangling chemical bonds at the interface of two semiconductors form interface states. Conduction and valence band discontinuities are affected by the dipole effect induced by electron transfer. Interestingly, the dipole effect is significantly reduced and becomes negligible if there is large lattice mismatch, as is the case with a ZnO/Si heterojunction [22]. Therefore, Anderson's rule is valid to determine the band edge offsets of a highly mismatched ZnO/Si heterojunction.

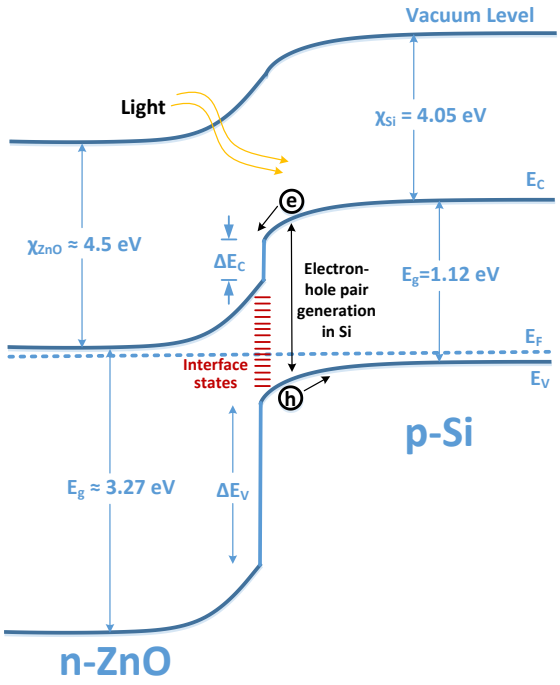

Figure 2. Schematic diagram of n-ZnO/p-Si heterojunction band-bending. χ denotes electron affinity of the material mentioned in the subscript.

When a photon gets absorbed in *p*-Si after being transmitted through a wide bandgap in *n*-ZnO, it generates an electron, a minority carrier, in the conduction band, as shown in Figure 2. The minority carrier current plays a vital role in solar cell performance. For an applied bias voltage V_b, the electron minority carrier current is given by [23]

$$J_n = \frac{J_{n0}}{(1+\upsilon)}\left(exp\left(\frac{qV_b}{kT}\right)\right), \tag{3}$$

where

$$J_{n0} = kT\frac{\mu_{n1}}{L_{n1}}n_1, \tag{4}$$

and μ_n, L_n, and n_1 denote minority-carrier mobility, diffusion length, and concentration, respectively. The subscript 1 represents the depletion region extended in p-type material (Si in our case). The factor 'υ' appearing in Equation (3) defines the influence of the conduction band offset (ΔE_C) on the minority carrier electron current and is given by

$$\upsilon = \frac{1}{L_{n1}} \int_{x1}^{x2} \left(\frac{\mu_{n1} N_{c1}}{\mu_n N_c} \right) exp\left(-\frac{E_{c1} - E_c + q\Psi}{kT} \right) dx, \tag{5}$$

where $x_1 < 0$ to $x_2 > 0$ is the depletion region extended from Si to ZnO, and $\Psi(x)$ is the potential function. The subscripts 1 and 2 here represent Si and ZnO material respectively. The abrupt *pn* heterojunction with applied bias near-zero, Equation (5) can be solved to get

$$\upsilon = \frac{I_{v1}}{L_{n1}} + \frac{1}{L_{n1}} \left(\frac{\mu_{n1} N_{c1}}{\mu_{n2} N_{c2}} \right) I_{v2} exp\left(-\frac{E_{c1} - E_{c2}}{kT} \right), \tag{6}$$

where

$$I_{v1} = \int_{x1}^{0} exp\left(\frac{q\Psi(x)}{kT} \right) dx, \tag{7}$$

and

$$I_{v2} = \int_{0}^{x2} exp\left(\frac{q\Psi(x)}{kT} \right) dx. \tag{8}$$

The potential function can be supposed to be decoupled from the carrier transport equations and it satisfies Poisson's equation as

$$\frac{d^2\Psi}{dx^2} = -\frac{\rho(\Psi)}{\epsilon}, \tag{9}$$

where ρ is charge distribution and ϵ is the permittivity of the medium. The electrostatic potential $\Psi(x)$ obtained from Equation (9) can be used to solve Equations (3)−(8) for a wide bandgap *n*-layer (ZnO) on a narrow bandgap *p*-layer (Si) to get [24]

$$J_n = kT \frac{\mu_{n1} N_{c2} n_{i1}^2}{I_{v2} N_{c1} N_A} exp\left(-\frac{|\Delta E_c|}{kT} \right) \left(exp\left(\frac{qV}{kT} \right) - 1 \right), \tag{10}$$

which proves that for a wide bandgap n-layer on a narrow bandgap p-layer heterojunction, the minority carrier current J_n prominently decreases due to the conduction band offset ΔE_C. The simulation results demonstrated in Section 3.1 (Figure 3) confirm this phenomena.

3. Results and Analysis

We prepared ZnO thin films using RF sputtering and performed detailed characterization. The experimental details have been reported elsewhere [25]. The photoluminescence and absorption measurements performed in our labs showed a bandgap value of 3.27 eV, which was used in the simulation. The most common value of electron affinity (4.5 eV) provided in literature was used initially. The absorption spectrum of ZnO of thickness ~0.5 µm measured in our lab using the Filmetrics tool was used in the simulation to investigate the effect of electron affinity. The details of the n-ZnO/p-Si solar cell modeling, structure schematic, and other optimized parameters for PC1D can be found in earlier reports [1,26].

3.1. Personal Computer One Dimensional (PC1D) Simulations

In the photovoltaic community, PC1D is a popular software package to simulate optical and electrical behavior of solar cell devices. This software was originally developed in the 1980s by Basore et al. [27] and has been continuously improved alongside progress in experimental work and theoretical models [28].

Figure 3 illustrates PC1D based simulation results of improvement in efficiency with reduction in electron affinity of ZnO. It is obvious that the conversion efficiency exceeds 20% by lowering electron affinity to 4.3 eV. The reason behind this phenomenon is reduction in conduction band offset ΔE_C that leads to an increase in minority-carrier current J_n as proved by Equation (10). Another factor contributing to improved efficiency is the decrease in the dark current. In other words, when a barrier for majority carrier electrons is formed by conduction band offset, it increases the probability of recombination via interface defects by the Shottky-Read-Hall (SRH) mechanism. The maximum efficiency of 20.34% can be achieved with ZnO having a bandgap of 3.27 eV and electron affinity of ~4.1 eV. Further reduction in electron affinity deteriorates cell efficiency. This can be theoretically confirmed by the band-bending diagram of the ZnO/Si junction as shown in Figure 4. Since the electron affinity of Si is ~4.05 eV, the electron affinity of ZnO below this value results in formation of a spike in the conduction band of the n-ZnO region. This spike acts as a potential barrier and blocks electron flow from the p-Si to the n-ZnO region. Therefore, it is difficult for the p-Si region to contribute to the photocurrent. This reasoning is supported by Figure 5 which depicts significant increase in V_{OC} with reduction in electron affinity. A negligible increase in J_{SC} can be attributed to the same reason.

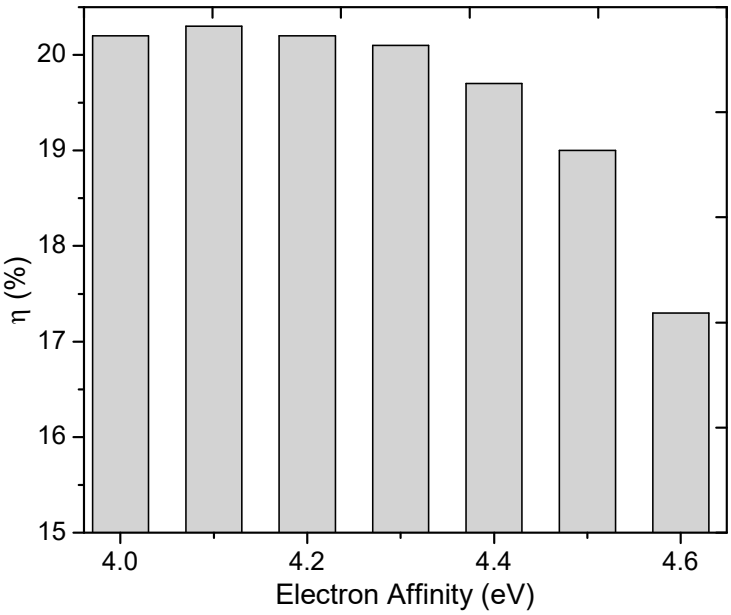

Figure 3. Influence of electron affinity of ZnO (bandgap: 3.27 eV) on the efficiency of n-ZnO/p-Si heterojunction solar cell using PC1D simulations.

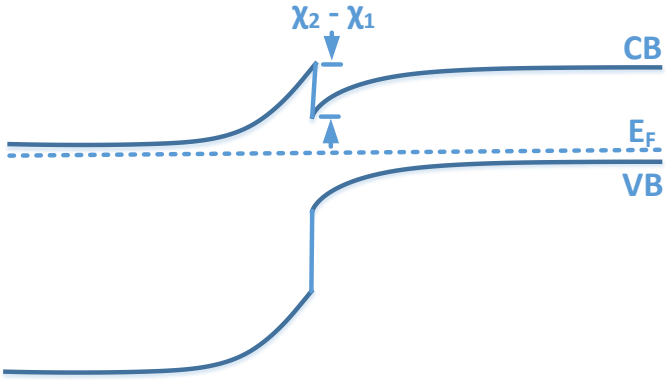

Figure 4. Schematic of the band-bending when electron affinity of ZnO (χ_1), at left, is lower than that of Si (χ_2), at right. CB: conduction band, VB: valence band, E_F: fermi level.

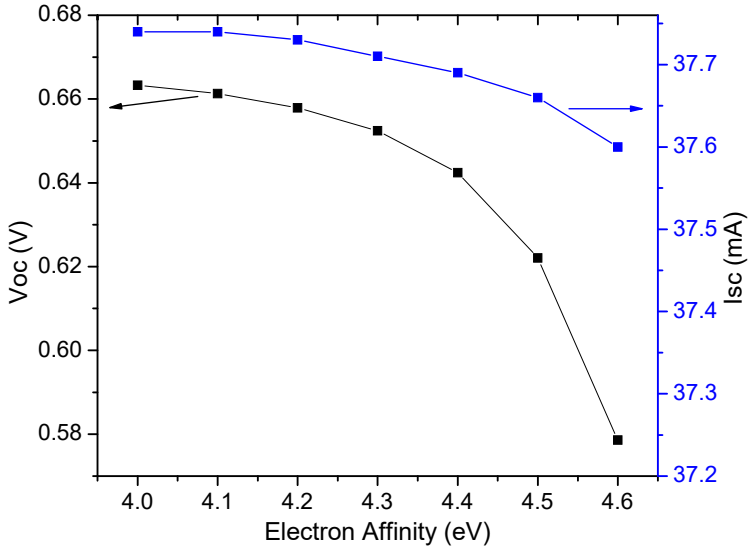

Figure 5. Effect of electron affinity of ZnO (bandgap: 3.27 eV) on the V_{OC} and I_{SC} of n-ZnO/p-Si solar cell using PC1D simulations.

The efficiency of the solar cell alters by modifying the bandgap as well. The change in conversion efficiency with a bandgap value of ZnO is shown in Figure 6 for three different values of electron affinity. The absorption spectrum was altered for values of bandgap other than 3.27 eV to get realistic results. The efficiency increases by decreasing the bandgap (or valence-band off-set). This improvement in efficiency cannot be explained using a band-bending diagram based on the famous Anderson's rule which ignores the effects of chemical bonding. The chemical bonding or electrical polarization due to interface states can alter the band bending significantly. Figure 6 also illustrates that the efficiency reduces significantly below a certain bandgap value. It is predictable because a considerable part of the solar spectrum gets absorbed in ZnO for such a small bandgap value. The ZnO layer is much thinner (0.5 μm) than Si (160 μm), but it has a higher absorption coefficient due to the direct bandgap of ZnO.

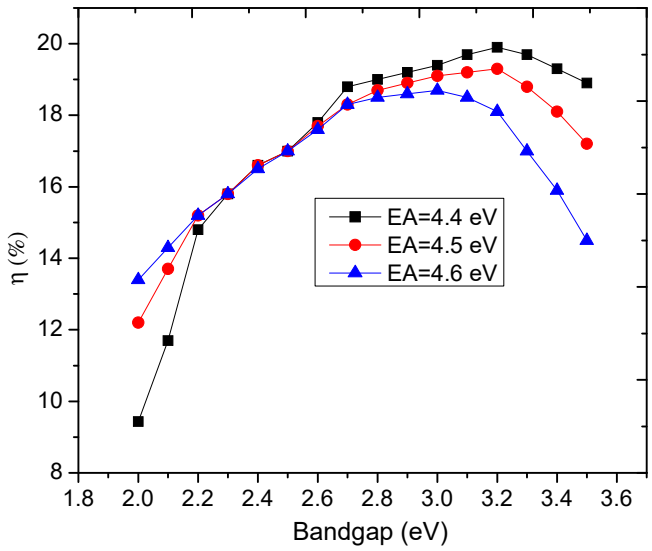

Figure 6. Change in overall conversion efficiency of n-ZnO/p-Si solar cell with modification of bandgap value of ZnO for three different values of electron affinity (EA). Few data points have been interpolated because numerical solution was not converging for those points in PC1D.

We have grown Ga rich ZnO:Ga films using MOCVD to examine the bandgap tuning. Trimethylgallium was used as the Ga source. The experimental details are provided elsewhere [1].

The photoluminescence (PL) spectra of both ZnO and ZnO:Ga were dominated by the near band edge (NBE) emission. The bandgap was blue-shifted by ~105 meV (12 nm). The molar ratio of Ga was ~50% during our growth process which lead to a bandgap of around 3.35 eV (370 nm). This is in accordance with the model reported by Zhao et al. [29]. We attribute this increase in the bandgap of ZnO to the well-known Burstein-Moss effect in which effective bandgap of a heavily doped semiconductor is increased as the absorption edge in the conduction band moves to higher energies because all states close to the conduction band edge are filled.

4. Conclusions

It is ascertained using PC1D simulations that the open circuit voltage of a n-ZnO/p-Si single heterojunction solar cell can be significantly improved by tuning the bandgap and/or electron affinity of ZnO by doping or alloying. The experimentally measured bandgap and absorption spectrum of ZnO was used in simulations using modified PC1D software. The major reasons for improvement in the solar cell efficiency are reduced conduction band offset that results in an increase in the minority carrier current and reduction in the dark current. The best values calculated for open circuit voltage, short circuit current density, fill factor, and conversion efficiency are 0.662 V, 37.7 mA/cm^2, 0.815, and 20.34%, respectively, for ZnO having a bandgap of 3.27 eV and electron affinity of 4.1 eV.

Author Contributions: Conceptualization, B.H.; methodology, B.H. and A.A.; software, B.H. and A.A.; validation, M.C. and T.M.K.; writing—original draft preparation, B.H. and A.A.; writing—review and editing, M.C., B.Z., and T.M.K.; visualization, B.Z. and A.A.

Funding: This research received no external funding.

Acknowledgments: The first author is thankful to Dr. Michael Fiddy from UNC Charlotte for his kind help and guidance during this research.

Conflicts of Interest: The authors declare no conflicts of interest.

References

1. Hussain, B.; Ebong, A.; Ferguson, I. Zinc oxide as an active n-layer and antireflection coating for silicon based heterojunction solar cell. *Sol. Energy Mater. Sol. Cells* **2015**, *139*, 95–100. [CrossRef]
2. Baturay, S.; Ocak, Y.S.; Kaya, D. The effect of Gd doping on the electrical and photoelectrical properties of Gd:ZnO/p-Si heterojunctions. *J. Alloys Compd.* **2015**, *645*, 29–33. [CrossRef]
3. Ren, X.; Zi, W.; Ma, Q.; Xiao, F.; Gao, F.; Hu, S.; Zhou, Y.; Liu, S.F. Topology and texture controlled ZnO thin film electrodeposition for superior solar cell efficiency. *Sol. Energy Mater. Sol. Cells* **2015**, *134*, 54–59. [CrossRef]
4. Zeng, X.; Wen, X.; Sun, X.; Liao, W.; Wen, Y. Boron-doped zinc oxide thin films grown by metal organic chemical vapor deposition for bifacial a-Si:H/c-Si heterojunction solar cells. *Thin Solid Films* **2016**, *605*, 257–262. [CrossRef]
5. Das, S.C.; Green, R.J.; Podder, J.; Regier, T.Z.; Chang, G.S.; Moewes, A. Band Gap Tuning in ZnO Through Ni Doping via Spray Pyrolysis. *J. Phys. Chem. C* **2013**, *117*, 12745–12753. [CrossRef]
6. Mayer, M.A.; Speaks, D.T.; Yu, K.M.; Mao, S.S.; Haller, E.E.; Walukiewicz, W. Band structure engineering of ZnO1-xSex alloys. In *Proceedings of SPIE Volume 7770, Solar Hydrogen and Nanotechnology V, San Diego, CA, USA, 24 August 2010*; SPIE: Bellingham, WA, USA. [CrossRef]
7. Mayer, M.A.; Yu, K.M.; Haller, E.E.; Walukiewicz, W. Tuning structural, electrical, and optical properties of oxide alloys: ZnO1−xSex. *J. Appl. Phys.* **2012**, *111*, 113505. [CrossRef]
8. Untila, G.; Kost, T.; Chebotareva, A. Bifacial 8.3%/5.4% front/rear efficiency ZnO:Al/n-Si heterojunction solar cell produced by spray pyrolysis. *Sol. Energy* **2016**, *127*, 184–197. [CrossRef]
9. Ahmmed, S.; Aktar, A.; Kuddus, A.; Ismail, A.B.M. Fabrication of Thin-Film Solar Cell using Spin Coated Zinc Oxide and Silicon Nanoparticles Doped Cupric Oxide Heterojunction. In Proceedings of the 2018 International Conference on Computer, Communication, Chemical, Material and Electronic Engineering (IC4ME2), Rajshahi, Bangladesh, 8–9 February 2018; pp. 1–4.

10. Chen, L.; Chen, X.; Liu, Y.; Zhao, Y.; Zhang, X. Research on ZnO/Si heterojunction solar cells. *J. Semicond.* **2017**, *38*, 054005. [CrossRef]
11. Shokeen, P.; Jain, A.; Kapoor, A. Embedded vertical dual of silver nanoparticles for improved ZnO/Si heterojunction solar cells. *J. Nanophoton* **2017**, *11*, 1. [CrossRef]
12. Hussain, B. Improvement in open circuit voltage of n-ZnO/p-Si solar cell by using amorphous-ZnO at the interface. *Prog. Photovolt: Res. Appl.* **2017**, *25*, 919–927. [CrossRef]
13. Pietruszka, R.; Witkowski, B.; Zielony, E.; Placzek-Popko, E.; Godlewski, M.; Gwozdz, K. ZnO/Si heterojunction solar cell fabricated by atomic layer deposition and hydrothermal methods. *Sol. Energy* **2017**, *155*, 1282–1288. [CrossRef]
14. Ziani, N.; Belkaid, M.S. Computer modeling zinc oxide/silicon heterojunction solar cells. *J. Nano Electron. Phys.* **2018**, *10*, 06002. [CrossRef]
15. Vallisree, S.; Thangavel, R.; Lenka, T.R. Modelling, simulation, optimization of Si/ZnO and Si/ZnMgO heterojunction solar cells. *Adv. Mater. Express* **2019**, *6*, 1–20. [CrossRef]
16. Askari, S.S.A.; Kumar, M.; Das, M.K. Numerical study on the interface properties of a ZnO/c-Si heterojunction solar cell. *Semicond. Sci. Technol.* **2018**, *33*, 1–8. [CrossRef]
17. Sundaram, K.B. Work function determination of zinc oxide films. *J. Vac. Sci. Technol. A: Vac. Surf. Films* **1997**, *15*, 428–430. [CrossRef]
18. Jiang, X.; Jia, C.L.; Szyszka, B. Manufacture of specific structure of aluminum-doped zinc oxide films by patterning the substrate surface. *Appl. Phys. Lett.* **2002**, *80*, 3090–3092. [CrossRef]
19. Lee, J.; Choi, Y.; Kim, J.; Park, M.; Im, S. Optimizing n-ZnO/p-Si heterojunctions for photodiode applications. *Thin Solid Films* **2002**, *403*, 553–557. [CrossRef]
20. Lee, J.; Choi, Y.; Choi, W.; Yeom, H.; Yoon, Y.; Kim, J.; Im, S. Characterization of films and interfaces in n-ZnO/p-Si photodiodes. *Thin Solid Films* **2002**, *420*, 112–116. [CrossRef]
21. Shih, J.-L. Zinc oxide-silicon heterojunction solar cells by sputtering. Master's Thesis, McGill University, Montreal, QC, Canada, November 2007; p. 118.
22. Ruan, Y.-C.; Ruan, Y.; Ching, W.Y. An effective dipole theory for band lineups in semiconductor heterojunctions. *J. Appl. Phys.* **1987**, *62*, 2885–2897. [CrossRef]
23. Gopal, V.; Singh, S.; Mehra, R. Analysis of dark current contributions in mercury cadmium telluride junction diodes. *Infrared Phys. Technol.* **2002**, *43*, 317–326. [CrossRef]
24. Kraut, E.A. The effect of a valence-band offset on potential and current distributions in HgCdTe heterostructures. *J. Vac. Sci. Technol. A: Vac. Surf. Films* **1989**, *7*, 420–423. [CrossRef]
25. Hussain, B.; Ali, A.; Unsur, V.; Ebong, A. On structural and electrical characterization of n-ZnO/p-Si single heterojunction solar cell. In Proceedings of the 2016 IEEE 43rd Photovoltaic Specialists Conference (PVSC), Portland, OR, USA, 5–10 June 2016; pp. 1898–1901.
26. Hussain, B. Development of n-ZnO/p-Si single heterojunction solar cell with and without interfacial layer. Ph.D. Thesis, The University of North Carolina at Charlotte, Charlotte, NC, USA, 2017; p. 154.
27. Basore, P. Numerical modeling of textured silicon solar cells using PC-1D. *IEEE Trans. Electron Devices* **1990**, *37*, 337–343. [CrossRef]
28. Clugston, D.; Basore, P. PC1D version 5: 32-bit solar cell modeling on personal computers. In Proceedings of the Conference Record of the Twenty Sixth IEEE Photovoltaic Specialists Conference – 1997, Anaheim, CA, USA, 29 September–3 October 1997. [CrossRef]
29. Zhao, J.; Sun, X.W.; Tan, S.T. Bandgap-Engineered Ga-Rich GaZnO Thin Films for UV Transparent Electronics. *IEEE Trans. Electron Devices* **2009**, *56*, 2995–2999. [CrossRef]